

STUDY OF DARK-MATTER ADMIXED NEUTRON STARS USING THE EQUATION OF STATE FROM THE ROTATIONAL CURVES OF GALAXIES

Z. REZAEI

Physics Department and Biruni Observatory
College of Sciences, Shiraz University
Shiraz 71454, Iran

ABSTRACT

In this work, we employ the dark matter equations of state (DMEOSs) obtained from the rotation curves of galaxies as well as the fermionic DMEOS with $m = 1.0 \text{ GeV}$ to study the structure of dark-matter admixed neutron stars (DMANSs). Applying the equation of state in the Skyrme framework for the neutron matter, we calculate the mass-radius relation for different DMANSs with various DMEOSs and central pressure of dark matter to neutron matter ratios. Our results show that for some DMEOSs, the mass-radius relations are in agreement with the new observations, e.g. EXO 1745-248, 4U 1608-52, and 4U 1820-30, which are inconsistent with the normal neutron stars. We conclude that both DMEOS and central pressure ratio of dark matter to neutron matter affect the slope of the mass-radius relation of DMANS. This is because of the interaction between dark matter and neutron matter which leads to gravitationally or self bound DMANSs. We study the radius of the neutron matter sphere as well as the radius of the dark matter halo for different DMANSs. The results confirm that in some cases, the neutron matter sphere with a small radius is surrounded by a halo of dark matter having a larger radius. Our calculations verify that due to the different degrees of dark matter domination in DMANSs, with a value of the visible radius of star two possible DMANSs with different masses can be exist. The gravitational redshift is also calculated for DMANSs with different DMEOSs and central pressure ratios. The results explain that the existence of dark matter in the DMANS leads to higher values for the gravitational redshift of the star.

Keywords: stars: neutron - dark matter - galaxies: halos - galaxies: kinematics and dynamics - equation of state.

1. INTRODUCTION

Neutron star is a compact star which contains plenty of neutrons. The theory of general relativity predicts the existence of a maximum mass above which the neutron star is unstable and collapses into a quark star or black hole. The maximum mass of neutron star depends on the interaction between particles and thus the equation of state (EOS) of the system. The stiffer the equation of state, the larger the maximum mass of neutron star. In addition, the rotation of neutron star leads to the higher values for the maximum mass. Since the neutron star contains dense asymmetric nuclear matter, one should apply the EOS of strongly interacting asymmetric nuclear matter to investigate the bulk properties of star. Besides, some authors have studied the effects of the existence of other particles such as hyperons, meson condensates, and quarks in the core of neutron star on the maximum mass (Ozel 2006; Alford et al. 2007; Li et al. 2010).

From the observation, the radio pulsars show large masses about $2 M_{\odot}$ (Ozel 2006; Demorest et al. 2010; Antoniadis et al. 2013). For example, according to (Ozel 2006), for the neutron star EXO 07482676 the mass is measured to be $2.10 \pm 0.28 M_{\odot}$ and the radius equals to $13.8 \pm 1.8 \text{ km}$. From the theory, stiff EOSs like the neutron matter equation of state in SLy230a and SLy230b models (Chabanat et al. 1997), can result in such large masses and mass-radius relations. Nevertheless, in some observations such as EXO 1745-248 with the mass $M = 1.4 \pm 0.1 M_{\odot}$ and the radius $R = 11 \pm 1 \text{ km}$ (Ozel & Guver & Psaltis 2009), the neutron star in 4U 1608-52 with the mass $M = 1.74 \pm 0.14 M_{\odot}$ and the radius $R = 9.3 \pm 1.0 \text{ km}$ (Guver et al. 2010A), and also the neutron star in the low-mass X-ray binary 4U 1820-30 with the mass $M = 1.58 \pm 0.06 M_{\odot}$ and the radius $R = 9.1 \pm 0.4 \text{ km}$ (Guver et al. 2010B), the results are different. It can be shown that soft EOSs are needed to lead these mass-radius relations from the

observation. Different equations of state for pure nuclear matter which have been obtained using different methods such as variational method with AV_{18} potential plus the UIX potential or AV_{18} potential plus a three-body UIX potential (Akmal & Pandharipande 1997) and Dirac-Brueckner-Hartree-Fock models (Engvik et al. 1994; Prakash et al. 1988) can not predict some observational data such as 4U 1608-52 and 4U 1820-30 (Lattimer & Prakash 2001, 2007). Therefore, this rules out the possibility of the existence of the pure nuclear matter in the neutron star. One explanation for these observations is that the existence of some particles such as quarks, mesons, and hyperons in the neutron star can lead to the soft equation of state and the mass-radius relations in agreement with these observations (Weber 2005; Page & Reddy 2006; Alford et al. 2007; Klahn et al. 2007).

In addition, another possibility that leads to these mass-radius relations is the existence of dark matter in the neutron star. Cosmological structure (Springel et al. 2005), gravitational lensing (Massey et al. 2007), and galactic rotation curve (Weber & de Boer 2010) are some observational reasons to confirm the existence of dark matter. According to (Ade et al. 2014), the contribution of ordinary matter, dark matter, and dark energy in the universe are 4.9%, 26.8%, and 68.3%, respectively. Supposing the existence of dark matter, it should be present in all astrophysical objects (Sandin & Ciarcelluti 2009). The dark matter may be accreted to the neutron stars because of the large density of the neutron star matter (Bertone & Fairbairn 2008; Perez-Garcia & Silk 2012; Fuller & Ott 2015). Therefore, to study the models of dark matter, neutron stars are much of interest in astrophysics and astroparticle physics (Goldman & Nussinov 1989; Bertone & Fairbairn 2008; Kouvaris 2012). It has been shown that self-annihilating neutralino WIMP dark matter accreted onto neutron stars may lead to seed compact objects with long-lived lumps of strange quark matter (Perez-Garcia & Silk & Stone 2010). The heating caused by possible dark matter (DM) annihilation in neutron stars may be an observable (Lavallaz & Fairbairn 2010) since the neutron star itself does not burn. In addition, it has been indicated that self-annihilation of DM in the neutron stars can change their linear and angular momentum (Perez-Garcia & Silk 2012) as well as the cooling properties of neutron stars (Kouvaris 2008). The critical phases of stellar evolution could be modified in the presence of relatively small amounts of DM (Sandin & Ciarcelluti 2009).

Because of the possibility of the existence of dark matter in the neutron stars, a model called dark-matter admixed neutron star (DMANS) has been considered (Sandin & Ciarcelluti 2009; Ciarcelluti & Sandin 2011; Leung & Chu & Lin 2011, 2012; Xiang et al. 2014). The mechanisms for accumulating dark matter in neutron star can result both from the stellar formation process and from subsequent accumulation by accretion of dark matter particles during the stellar lifetime (Ciarcelluti & Sandin 2011). The dark matter inside the stars alters the structure and may lead to the collapse of a neutron star (Kouvaris 2012). The structure of these stars is still an open issue because of the unknown nature of dark matter. However, it is useful to study the structure of DMANSs using the existing information about the dark matter. The dark-matter admixed neutron star is a two-fluid system where the neutron star matter and dark matter interact only through gravitational force (Leung & Chu & Lin 2012). In order to study the structure of these stars, the Tolman- Oppenheimer-Volkoff (TOV) equation is separated into two different sets for the neutron star and dark components inside the star (Lavallaz & Fairbairn 2010; Sandin & Ciarcelluti 2009; Ciarcelluti & Sandin 2011; Leung & Chu & Lin 2011, 2012).

The mass-radius relation of DMANS which is affected by the dark matter is one of the observational results which is possible to measure. The basic equation for dark matter to study the structure of DMANS is the dark matter equation of state (Sandin & Ciarcelluti 2009; Ciarcelluti & Sandin 2011; Leung & Chu & Lin 2011; Xiang et al. 2014). Applying a method that combines kinematic and gravitational lensing data to test the widely adopted assumption of pressureless dark matter, the dark matter equation of state has been measured (Serra & Dominguez Romero 2011). Moreover, by modeling galactic halos describing the dark matter as a non zero pressure fluid and using observational data of the rotation curves of galaxies, a dark matter equation of state has been obtained (Barranco & Bernal & Nunez 2015).

Some studies have been done to investigate the structure of DMANSs (Sandin & Ciarcelluti 2009; Ciarcelluti & Sandin 2011; Leung & Chu & Lin 2011, 2012; Li & Huang & Xu 2012; Xiang et al. 2014). The general-relativistic hydrostatic equations were generalized to spherical objects with multiple fluids that interact by gravity (Sandin & Ciarcelluti 2009). Moreover, assuming that the microphysics is the same in the two sectors of the DMANSs, the effects of mirror dark matter on neutron star structure have been studied. It was concluded that the structure depends on the relative number of mirror baryons to ordinary baryons. Supposing that dark matter is made of some form of stable and long-living particles that can accumulate in the star, it has been shown that all mass-radius measurements can be explained with one nuclear matter equation of state and a dark core of varying relative size (Ciarcelluti & Sandin 2011). Consequently, observational data which provide a test of the theory, will become a powerful tool for the determination of dark matter (Ciarcelluti & Sandin 2011). Considering non-self-annihilating dark matter particles of

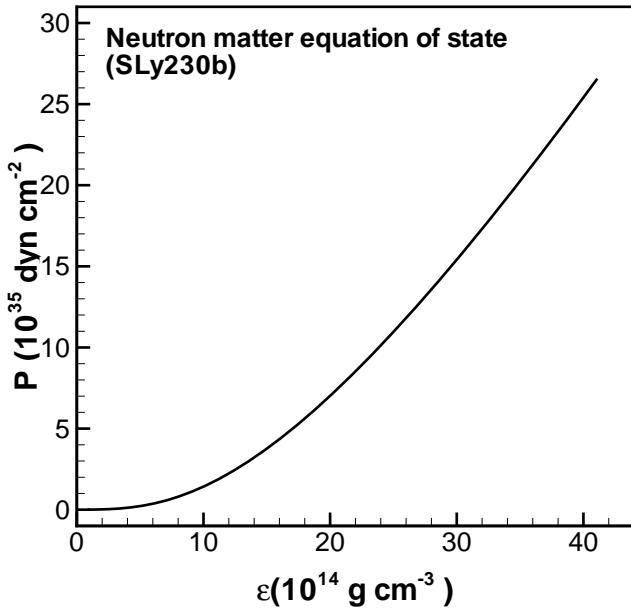


Figure 1. Neutron matter equation of state in the Skyrme framework, SLy230b (Chabanat et al. 1997).

mass 1.0 GeV along with normal nuclear matter and using a general relativistic two-fluid formalism, the properties of dark-matter admixed neutron stars have been studied (Leung & Chu & Lin 2011). It was found that a new class of compact stars consisting a small normal matter core with radius of a few km within a ten-kilometer- sized dark matter halo can exist. Employing a general relativistic two-fluid formalism to study the admixture of degenerate dark matter and normal nuclear matter shows that a new class of compact stars which are dominated by DM can exist (Leung & Chu & Lin 2012). These stars have a small neutron star matter core with radius a few km embedded in a larger ten-kilometer-sized DM halo. In addition, these DMANSs have two classes of oscillation modes. The first class of modes reduce to the same set of modes for ordinary neutron stars without DM and the second class of modes is due to dark matter. In a consistent DMANS model, considering dark matter particles to behave like fermions which interact with a certain repulsive interaction, it has been found that dark matter would soften the equation of state more strongly than that of hyperons, reducing the maximum mass of the star (Li & Huang & Xu 2012). However, with the small mass particles, the maximum mass could be larger than $2 M_{\odot}$. The effects of fermionic dark matter on the properties of neutron stars using the two-fluid Tolman-Oppenheimer-Volkoff formalism have been studied (Xiang et al. 2014). It has been shown that the mass of dark matter candidates, the amount of dark matter, and interactions among dark matter candidates affect the mass-radius relationship. In addition, the DM in DMANS results in a spread of mass-radius relationships, and in some cases, the DM distribution can surpass the neutron matter (NM) distribution to form DM halo. It has been confirmed that the DM admixture in neutron stars lead to the shrinkage of the NM surface which results in the small radius observation. Moreover, the DM distribution can surpass the neutron star matter distribution and form DM halo when the DM candidates have low mass or the repulsion of DM exists. It is while with the large DM fraction in the DMANSs, the repulsive interaction among DM may result in stars with the mass above $2 M_{\odot}$. In the present work, we investigate the properties of DMANSs using the Skyrme interaction in the neutron star matter and the dark matter equation of state obtained from the rotation curves of galaxies in a general relativistic two-fluid formalism.

2. FORMALISM

In this study, we employ the neutron matter equation of state which has been derived in the Skyrme framework (Chabanat et al. 1997). This equation is the result of the Skyrme effective force, SLy230b, with the improvement in the behavior with respect to the isospin degree of freedom (Chabanat et al. 1997). The EOS of neutron matter in the SLy230b parametrization has been presented in Figure 1. Recently, the dark matter equation of state has been presented using the velocity profile of galaxies (Barranco & Bernal & Nunez 2015). In this study, we apply the pseudo isothermal model in which the dark matter density profile determines the velocity profile (Barranco & Bernal & Nunez

2015). The equation of state for the Pseudo-Isothermal density profile is as follows (Barranco & Bernal & Nunez 2015),

$$p(\rho) = \frac{8p_0}{\pi^2 - 8} \left[\frac{\pi^2}{8} - \frac{\arctan \sqrt{\frac{\rho_0}{\rho} - 1}}{\sqrt{\frac{\rho_0}{\rho} - 1}} - \frac{1}{2} (\arctan \sqrt{\frac{\rho_0}{\rho} - 1})^2 \right]. \quad (1)$$

In the above equation, ρ and p are the density and pressure of dark matter, respectively. In addition, ρ_0 and p_0 are the only free parameters of the equation of state which for the dark matter in galaxies correspond to the central density and pressure, respectively (Barranco & Bernal & Nunez 2015). It has been found that this equation of state has a functional dependence universal for all galaxies and the mentioned free parameters are related with the evolution history of the galaxy. Using the equation of state in Eq. (1) and the rotational curve data, one can predict the central pressure and density of the galaxies. Here, we suppose that the dark matter in DMANSs also behaves according to this equation of state. However, one should be careful about the value of the free parameters ρ_0 and p_0 in the equation of state. A logical choice which is similar to the case of the galaxies, is that the values of ρ_0 and p_0 are with the order of the central density and pressure of neutron stars, respectively, i.e. $\sim 10^{15} g/cm^3$ for the density and $\sim 10^{36} dyn/cm^2$ for the pressure. We consider 12 EOSs with the value $\rho_0 = 0.3 \times 10^{16} g/cm^3$ and different values of p_0 , from 0.1×10^{35} to $4.0 \times 10^{35} dyn/cm^2$. These EOSs are presented in Figure 2. We should note that we have used the units in which $G = c = 1$ and therefore, the mass density and energy density of dark matter are equal, i.e. $\varepsilon = \rho$.

It is clear that the increase in the value of p_0 leads to more stiffness in the equation of state. Besides, it is possible to consider DMANSs in which the dark matter sector composed by free fermions with arbitrary masses (Narain et al. 2007). In this case, the equation of state at zero temperature, $p(\rho)$, is obtained as follows (Narain et al. 2007),

$$\rho = \frac{1}{\pi^2} \int_0^{k_F} k^2 \sqrt{m^2 + k^2} dk = \frac{m^4}{8\pi^2} [(2z^3 + z)(1 + z^2)^{1/2} - \sinh^{-1}(z)], \quad (2)$$

$$p = \frac{1}{3\pi^2} \int_0^{k_F} \frac{k^4}{\sqrt{m^2 + k^2}} dk = \frac{m^4}{24\pi^2} [(2z^3 - 3z)(1 + z^2)^{1/2} + 3\sinh^{-1}(z)]. \quad (3)$$

In the above equation, $k_F = (3\pi^2 n)^{1/3}$ denotes the Fermi momentum and n is the total number density of fermions. In addition, m shows the mass of fermions and $z = k_F/m$. The equation of state with the mass $m = 1.0 GeV$ for the fermions is presented in Figure 3.

In this work, we study a dark matter admixed neutron star with two concentric spheres one containing the neutron matter and the other the dark matter. The EOS of neutron matter in the neutron matter sphere is presented in Figure 1, and the EOSs of dark matter in the dark matter sphere are given in Figures 2 and 3. In our calculations for the neutron matter sphere, in the crust at densities lower than $0.05 fm^{-3}$, we use the equation of state calculated by Baym et al. (Baym et al. 1971). The contribution of dark matter in the DMANS can be different and depends on the history of the star (Sandin & Ciarcelluti 2009) and the way that it originates (Xiang et al. 2014). The gravitational field of the normal star in all phases of evolution can affect the dark matter and capture it into the star. This is more probable when the star is more compact. Besides, the opposite scenario in which the dark matter objects trap the baryons has been also proposed (Ciarcelluti & Sandin 2011). In this case, the more important contribution of dark matter in the DMANS is expected. In this study, we explore the DMANSs with different portions of dark matter in the center of DMANS. This will be done by considering different central pressure ratios, i.e. central dark matter pressure to central neutron matter pressure ratio $\delta = \frac{p_D(r=0)}{p_N(r=0)}$, for the DMANS. The zero pressure ratio, $\delta = 0$, shows a normal neutron star.

In our calculations of the DMANS structure, we apply the two-fluid formulism for the neutron and dark matter presented by (Ciarcelluti & Sandin 2011; Sandin & Ciarcelluti 2009). In this formalism, it is proposed that dark matter interacts with neutron matter just by gravity. One static and spherically symmetric space-time with the line element, (we use the units in which $G = c = 1$),

$$d\tau^2 = e^{2\nu(r)} dt^2 - e^{2\lambda(r)} dr^2 - r^2(d\theta^2 + \sin^2\theta d\phi^2), \quad (4)$$

and the energy-momentum tensor of a perfect fluid,

$$T^{\mu\nu} = -pg^{\mu\nu} + (p + \varepsilon)u^\mu u^\nu, \quad (5)$$

are considered. In the above equation, p and ε are the total pressure and total energy density, respectively. The total

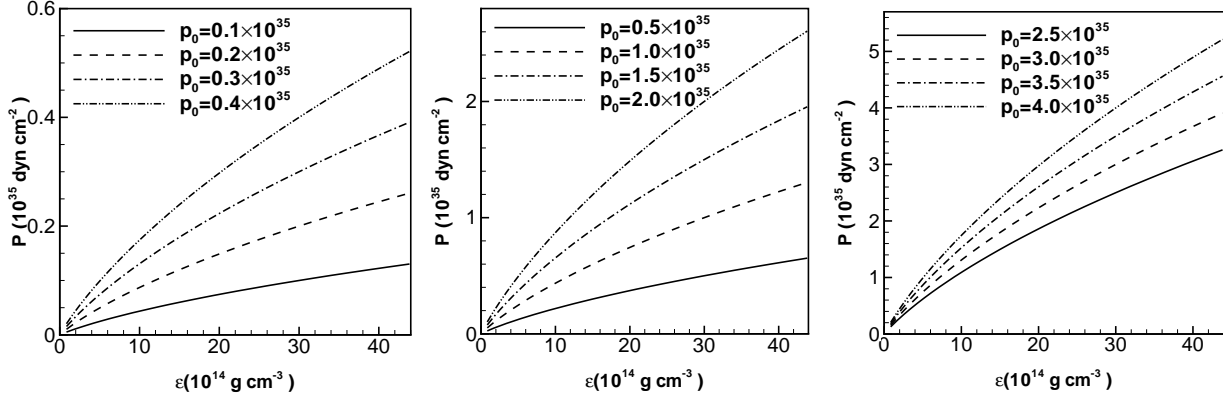


Figure 2. Dark matter equation of state from the velocity profile of galaxies with the value $\rho_0 = 0.3 \times 10^{16} g/cm^{-3}$ and different values of p_0 in dyn/cm^2 unit.

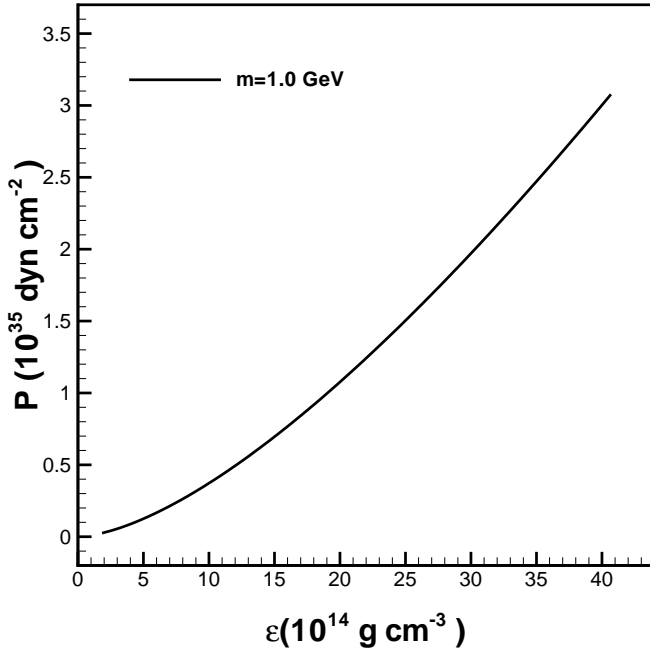


Figure 3. Equation of state for a free gas of fermions at zero temperature with the value of $m = 1.0 GeV$ for the mass of fermions.

energy density is related to the rest-mass energy density (ε_{rm}) and internal energy density (ε_{in}) by

$$\varepsilon = \varepsilon_{rm} + \varepsilon_{in}. \quad (6)$$

In our system, the total pressure and total energy density are the results of both neutron matter and dark matter portions,

$$p(r) = p_N(r) + p_D(r), \quad (7)$$

$$\varepsilon(r) = \varepsilon_N(r) + \varepsilon_D(r), \quad (8)$$

in which p_i and ε_i are the pressure and energy density of neutron ($i = N$) and dark ($i = D$) matter at position r from the center of the star, respectively. Applying some calculations, the Einstein field equations lead to (Sandin & Ciarcelluti 2009; Ciarcelluti & Sandin 2011; Xiang et al. 2014),

$$e^{-2\lambda(r)} = 1 - \frac{2M(r)}{r}, \quad (9)$$

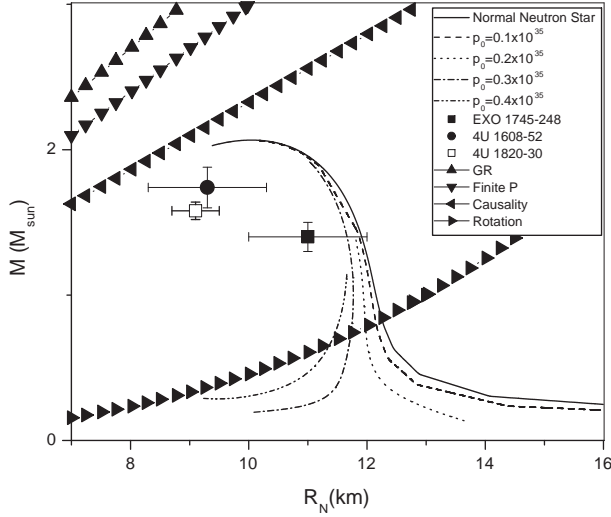


Figure 4. $M - R_N$ relation for normal neutron star and DMANSs with different values of p_0 in dyn/cm^2 unit for the case of $\delta = 1$ and some observational data. The curves that exclude some regions, i.e. by the general relativity $M > \frac{c^2 R}{2G}$ (GR), by the finite pressure $M > \frac{4}{9} \frac{c^2 R}{G}$ (Finite P), by causality $M > \frac{10}{29} \frac{c^2 R}{G}$ (Causality), and by the rotation of 716 Hz pulsar J1748-2446ad (Rotation), are also presented (Lattimer & Prakash 2007).

$$\frac{d\nu}{dr} = \frac{M(r) + 4\pi r^3 p(r)}{r[r - 2M(r)]}, \quad (10)$$

$$\frac{dp_N}{dr} = -[p_N(r) + \varepsilon_N(r)] \frac{d\nu}{dr}, \quad (11)$$

$$\frac{dp_D}{dr} = -[p_D(r) + \varepsilon_D(r)] \frac{d\nu}{dr}. \quad (12)$$

In above equations, r denotes the radial coordinate from the center of the star. In addition, $M(r) = \int_0^r dr 4\pi r^2 \varepsilon(r)$ is the total mass inside a sphere with radius r . This separation for dark matter and neutron matter is due to the assumption that the two sectors interact just by gravity. The structure of DMANS is described by these two-fluid Tolman-Oppenheimer-Volkoff (TOV) equations. The condition for the DMANS radius, R , and mass, $M(R)$, is $p(R) = 0$ (Xiang et al. 2014). Moreover, the radius and mass of the neutron matter sphere and dark matter sphere are determined with the conditions $p_N(R_N) = 0$ and $p_D(R_D) = 0$, respectively (Xiang et al. 2014). It should be noted that the radial dependencies of the pressure and density are different in the two sectors.

3. RESULTS AND DISCUSSION

Figures. 4-7 show the total mass of the DMANS versus the radius of the neutron matter sphere ($M - R_N$ relation) for normal neutron star and DMANSs with different dark matter equations of state (DMEOSs) when the central pressure of neutron and dark matter are the same, i.e. $\delta = 1$. The curves which apply constraints for the mass and radius, i.e. by the general relativity $M > \frac{c^2 R}{2G}$ (GR), by the finite pressure $M > \frac{4}{9} \frac{c^2 R}{G}$ (Finite P), by causality $M > \frac{10}{29} \frac{c^2 R}{G}$ (Causality), and by the rotation of 716 Hz pulsar J1748-2446ad (Rotation), are also presented (Lattimer & Prakash 2007). The mass-radius relations are acceptable that pass in the permitted region. We can see that with all DMEOSs, the radius of a DMANS is smaller than the radius of a normal neutron star with the same mass. This decrease of radius in DMANSs is in agreement with the previous results (Leung & Chu & Lin 2011, 2012; Xiang et al. 2014).

It is obvious that the $M - R_N$ relations obtained using DMEOSs corresponding with $p_0 \leq 0.2 \times 10^{35} \text{ dyn}/\text{cm}^2$ show a behavior like that of the normal neutron stars which are gravitationally bound. However, the other DMEOSs which are the stiffer equations of state, lead to the $M - R_N$ relations significantly different from the normal neutron stars. Such $M - R_N$ relations with different slope, representing the self-bound DMANSs, are the result of the interaction

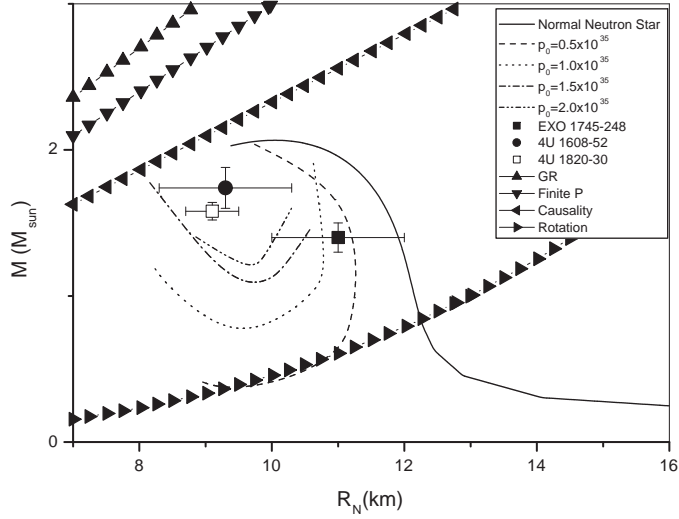


Figure 5. Same as Figure 4 but for other values of p_0 in dyn/cm^2 unit.

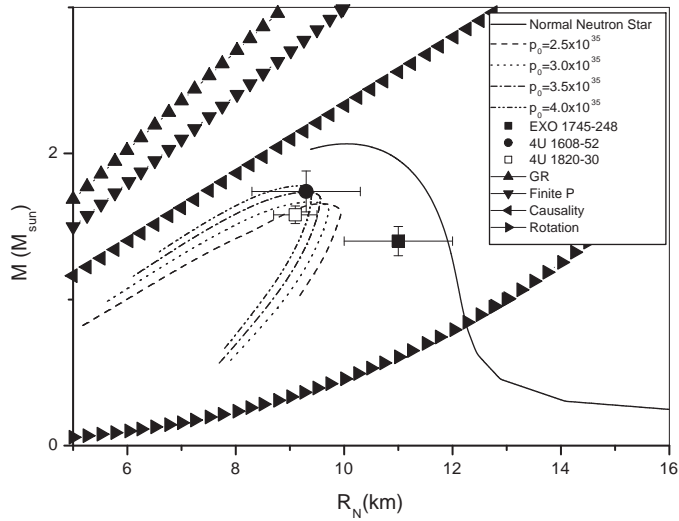


Figure 6. Same as Figure 4 but for other values of p_0 in dyn/cm^2 unit.

between dark matter and neutron matter. The significant effects of the stiff dark matter equations of state on $M - R_N$ relations has been also denoted in (Xiang et al. 2014). Our results indicate that the $M - R_N$ relation for the DMEOS with $p_0 = 0.5 \times 10^{35} \text{ dyn}/\text{cm}^2$ is approximately in agreement with the result related to the DMEOS with $m = 1.0 \text{ GeV}$. Figures. 4-7 show that for some $M - R_N$ relations, with a value of R_N two possible DMANSs with different masses can exist. This is a result of different degrees of dark matter domination in DMANSs. We mean that two equal sized DMANSs which are affected by the dark matter differently have various masses. For example, consider $M - R_N$ relation with $p_0 = 0.5 \times 10^{35} \text{ dyn}/\text{cm}^2$. With this DMEOS, two DMANSs with the similar radius 11.25 km and 11.36 km have masses of about $0.77M_\odot$ and $1.67M_\odot$, respectively. The ratio of the mass of dark matter sphere to the total mass for these two DMANSs are $\frac{M_D}{M} = 0.13$ and $\frac{M_D}{M} = 0.02$ respectively, indicating the more effect of dark matter in the first one. In addition, in the case of $m = 1.0 \text{ GeV}$, two DMANSs with radius 10.41 km and 10.39 km have mass $0.41M_\odot$ and $1.95M_\odot$, and the ratio of $\frac{M_D}{M}$ is 0.29 and 0.03 , respectively. The maximum mass of DMANS depends on the DMEOSs (see Table 1). We can see that with all DMEOSs, the maximum mass of DMANS is lower than the normal

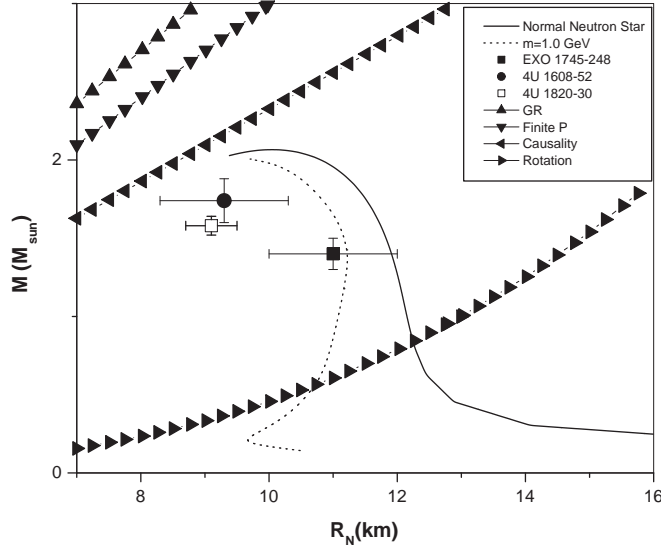


Figure 7. Same as Figure 4 but for the DMANS with the DMEOS given in Figure 3.

Table 1. The maximum masses and corresponding visible radii for normal neutron star and DMANSs with different dark matter equations of state for the case of $\delta = 1$.

	$M_{max}(M_{\odot})$	$R(km)$
Normal Neutron Star	2.07	10.04
$p_0(10^{35} dyn/cm^2)$		
0.1	2.06	10.18
0.2	1.39	11.80
0.3	1.92	11.02
0.4	1.16	11.66
0.5	2.05	9.71
1.0	1.91	10.63
1.5	1.78	8.16
2.0	1.60	10.30
2.5	1.68	9.35
3.0	1.68	9.38
3.5	1.74	9.25
4.0	1.78	9.11
$m(GeV)$		
1.0	2.01	9.70

neutron star. The decrease of the maximum mass due to the dark matter has been also reported in other studies (Leung & Chu & Lin 2011; Li & Huang & Xu 2012; Leung & Chu & Lin 2012; Xiang et al. 2014). Figures. 4-7 also show the comparison of observational data with the theoretical results. It is obvious that EXO 1745-248 with the mass $M = 1.4 \pm 0.1 M_{\odot}$ and the radius $R = 11 \pm 1 km$ can be hardly modeled with the normal neutron star. However, our model for DMANSs with $0.5 \times 10^{35} dyn/cm^2 \leq p_0 \leq 1.5 \times 10^{35} dyn/cm^2$ or with $m = 1.0 GeV$ can explain this observational result. The neutron star in 4U 1820-30 with $M = 1.58 \pm 0.06 M_{\odot}$ and $R = 9.1 \pm 0.4 km$ as well as the neutron star in 4U 1608-52 with $M = 1.74 \pm 0.14 M_{\odot}$ and $R = 9.3 \pm 1.0 km$ can not be normal neutron stars. It is clear that the DMEOSs with $2.5 \times 10^{35} dyn/cm^2 \leq p_0 \leq 4.0 \times 10^{35} dyn/cm^2$ corresponding to self-bound stars lead to the results in agreement with the properties of the neutron stars in 4U 1608-52 and 4U 1820-30.

Table 2 presents the mass and radius of the dark and neutron matter spheres related to the DMANSs with the

Table 2. The mass and radius of the dark and neutron matter spheres of the maximum mass DMANSs with different DMEOSs for the central pressure ratio $\delta = 1$.

	$M_D(M_\odot)$	$R_D(km)$	$M_N(M_\odot)$	$R_N(km)$	$M_{max}(M_\odot)$
$p_0(10^{35} \text{ dyn/cm}^2)$					
0.1	< 0.01	1.85	2.06	10.18	2.06
0.2	0.02	4.34	1.37	11.80	1.39
0.3	0.01	3.48	1.90	11.02	1.92
0.4	0.05	5.86	1.11	11.66	1.16
0.5	0.01	2.70	2.04	9.71	2.05
1.0	0.06	5.16	1.85	10.63	1.91
1.5	1.63	19.95	0.15	8.16	1.78
2.0	0.24	8.35	1.36	10.30	1.60
2.5	0.99	15.92	0.69	9.35	1.68
3.0	0.34	9.38	1.34	9.38	1.68
3.5	0.34	9.25	1.40	9.25	1.74
4.0	0.34	9.11	1.44	9.11	1.78
$m(GeV)$					
1.0	0.05	3.26	1.96	9.70	2.01

maximum mass. It can be seen that for DMANSs with DMEOSs corresponding to $p_0 \leq 1.0 \times 10^{35} \text{ dyn/cm}^2$, the significant contribution in the mass is related to the neutron matter sphere. Besides, in these cases, the radius of the dark matter sphere is smaller than the neutron matter sphere. Therefore, for $p_0 \leq 1.0 \times 10^{35} \text{ dyn/cm}^2$, the star is neutron matter dominated and gravitationally bound. However, in the DMANS with $p_0 \simeq 1.5 \times 10^{35} \text{ dyn/cm}^2$, the dark matter sphere with the mass $1.63 M_\odot$ is heavier than the neutron matter sphere with the mass $0.15 M_\odot$. In this star, the halo of dark matter with the radius 19.95 km surrounds the neutron matter sphere with smaller radius 8.16 km . This is a dark matter dominated neutron star. We can conclude from the above discussion that the neutron star EXO 1745-248 can be a dark matter dominated neutron star. Figures. 5 and 7 indicate that both DMEOSs $p_0 \simeq 1.0 \times 10^{35} \text{ dyn/cm}^2$ and $m = 1.0 \text{ GeV}$, which lead to self-bound DMANSs, can be used to explain the observational result EXO 1745-248. Moreover, Table 2 shows that the mass of dark matter sphere obtained from these two models, i.e. $0.06 M_\odot$ and $0.05 M_\odot$ respectively, are approximately the same. In addition, the DMEOS with $p_0 \simeq 2.5 \times 10^{35} \text{ dyn/cm}^2$ leads to the DMANS with a heavier and larger dark matter sphere compared to the neutron matter sphere. Consequently, this star is also a dark matter dominated neutron star. Therefore, the neutron stars 4U 1608-52 and 4U 1820-30 can be self-bound and dark matter dominated neutron stars. Table 2 indicates that the DMANSs with DMEOSs corresponding to $p_0 \geq 3.0 \times 10^{35} \text{ dyn/cm}^2$ are the stars with the more massive neutron matter sphere but the radii of two spheres are equal. By increasing the value of the free parameter p_0 from 3.0 to 4.0, the mass of the neutron matter sphere increases while the mass of the dark matter sphere remains constant with the value $0.34 M_\odot$. The increase in the value of p_0 reduces the radius of the neutron and dark matter spheres leading to the compactness of the star.

Figures. 8-10 show the $M - R_N$ relations with different DMEOSs for various central pressure ratios, δ . It is obvious that for all DMEOSs, when the central pressure ratio grows from 0.5 to 1, the low mass DMANSs (about $M \leq M_\odot$) will become more compact. This effect is more significant for the case of $m = 1.0 \text{ GeV}$. Besides, by increasing the central pressure ratio from 2 to 5, for DMANSs with $p_0 = 0.2 \times 10^{35} \text{ dyn/cm}^2$, the radius of star is not affected but the low mass DMANSs with $p_0 = 0.4 \times 10^{35} \text{ dyn/cm}^2$ and $m = 1.0 \text{ GeV}$ become more compact. The DMANSs with $m = 1.0 \text{ GeV}$ are more affected by the value of central pressure ratio compared to the cases with $p_0 = 0.4 \times 10^{35} \text{ dyn/cm}^2$. In the case with $m = 1.0 \text{ GeV}$, the DMANSs with the small central pressure ratios, i.e. $\delta \leq 0.75$, are like normal neutron stars and gravitationally bound. However, for higher values of central pressure ratio the DMANSs are self-bound stars. We have found from Figure. 9 that any DMANSs with the DMEOS $p_0 = 0.2 \times 10^{35} \text{ dyn/cm}^2$ and the central pressure ratios $\delta = 4.00$ and $\delta = 5.00$ do not exist. Figures. 8-10 confirm that the $M - R_N$ relation can be influenced significantly by the central pressure ratio like the results of (Xiang et al. 2014). The results for the maximum masses and corresponding radii are presented in Tables 3-5. It can be seen from Tables 3 and 4 that for DMANSs with $p_0 = 0.2 \times 10^{35} \text{ dyn/cm}^2$ and $\delta \geq 2$ as well as the DMANSs with $p_0 = 0.4 \times 10^{35} \text{ dyn/cm}^2$, the maximum mass decreases by increasing the central pressure ratio, in agreement with the results of (Xiang et al. 2014). Table 5 also

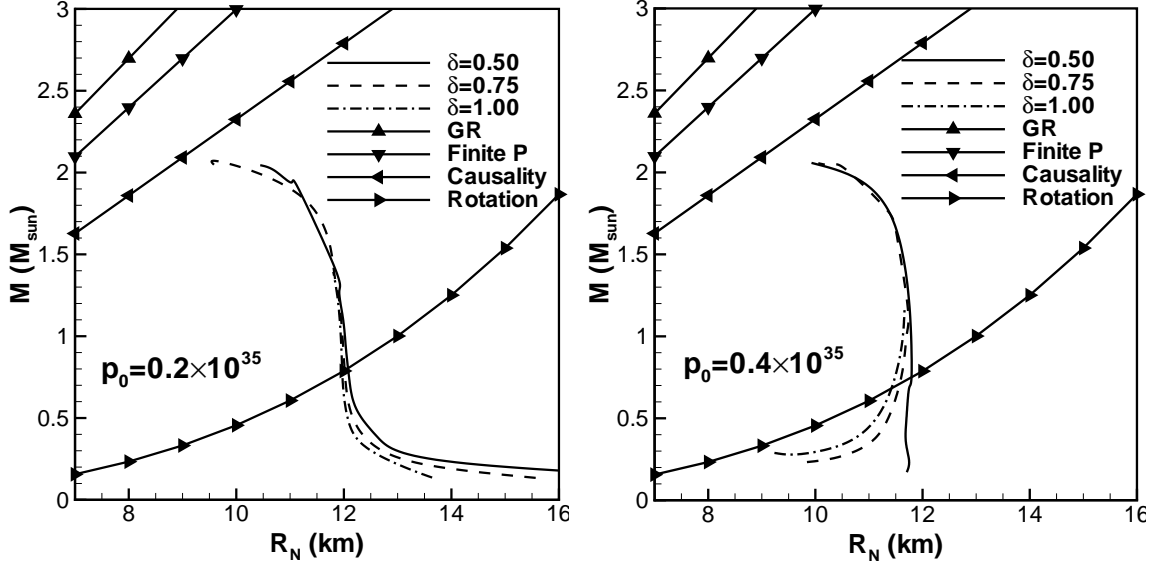


Figure 8. $M - R_N$ relations and constraint curves with two values of p_0 in dyn/cm^2 unit for different central pressure ratios, δ .

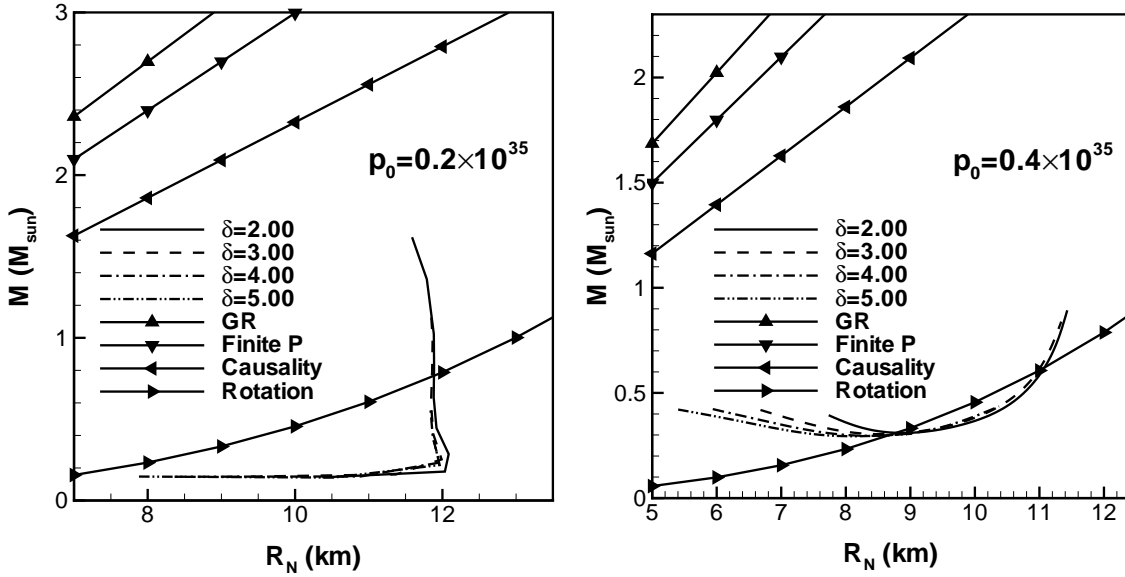


Figure 9. Same as Figure 8 but for other values of central pressure ratio, δ .

indicates that in the case with fermionic DMEOS, $m = 1.0 \text{ GeV}$, for $\delta > 1$ the maximum masses are smaller than the cases with $\delta < 1$.

The total mass versus the radius of the neutron and dark matter spheres for different DMEOSs and various values of central pressure ratio is given in Figures. 11-14. These figures show that for a DMANS with a specific mass, what size of the neutron and dark matter spheres is. We can see that for all values of central pressure ratio the radius of the neutron matter sphere of the star with $p_0 = 0.4 \times 10^{35} \text{ dyn}/\text{cm}^2$ is smaller than the case of $p_0 = 0.2 \times 10^{35} \text{ dyn}/\text{cm}^2$ with the same mass. However, it is clear that the radius of the dark matter sphere of the star with $p_0 = 0.4 \times 10^{35} \text{ dyn}/\text{cm}^2$ is larger compared to the case with $p_0 = 0.2 \times 10^{35} \text{ dyn}/\text{cm}^2$. Figures. 11-14 indicate that in the cases with $p_0 = 0.2 \times 10^{35} \text{ dyn}/\text{cm}^2$ and $p_0 = 0.4 \times 10^{35} \text{ dyn}/\text{cm}^2$ for $\delta \leq 3.0$ and in the case of $m = 1.0 \text{ GeV}$ for $\delta \leq 1.0$, the radius of the neutron matter sphere is larger than the radius of the dark matter one. The difference between the radius of the neutron and dark matter spheres is larger in stars with $p_0 = 0.2 \times 10^{35} \text{ dyn}/\text{cm}^2$ compared to the case of $p_0 = 0.4 \times 10^{35} \text{ dyn}/\text{cm}^2$. For all DMEOSs by increasing the central pressure ratio, the radius of the neutron matter sphere decreases while the radius of the dark matter sphere increases. For stars with $p_0 = 0.4 \times 10^{35} \text{ dyn}/\text{cm}^2$ and $\delta \geq 3.00$ as well as stars

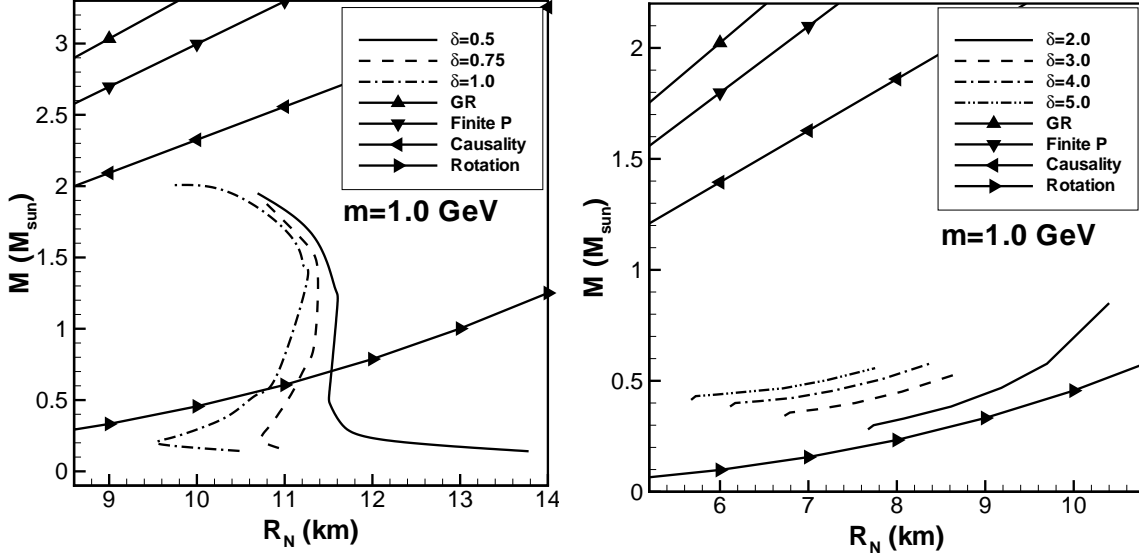


Figure 10. $M - R_N$ relations and constraint curves with the fermionic DMEOS for different central pressure ratios, δ .

Table 3. The maximum masses and corresponding visible radii for DMANSs with DMEOS corresponding to $p_0 = 0.2 \times 10^{35} \text{ dyn/cm}^2$ and different values of central pressure ratio, δ . In this case, any DMANSs with $\delta \geq 4.00$ do not exist.

δ	$M_{max}(M_{\odot})$	$R(km)$
0.50	2.05	10.44
0.75	2.06	9.81
1.00	1.39	11.80
2.00	1.62	11.59
3.00	1.18	11.84

Table 4. Same as Table 3 but for DMANSs with DMEOS corresponding to $p_0 = 0.4 \times 10^{35} \text{ dyn/cm}^2$.

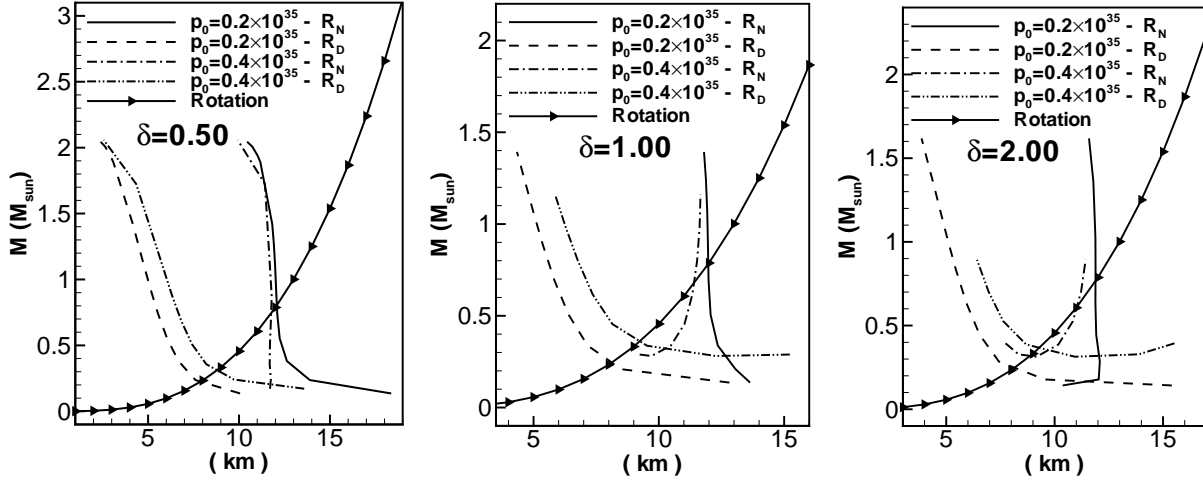
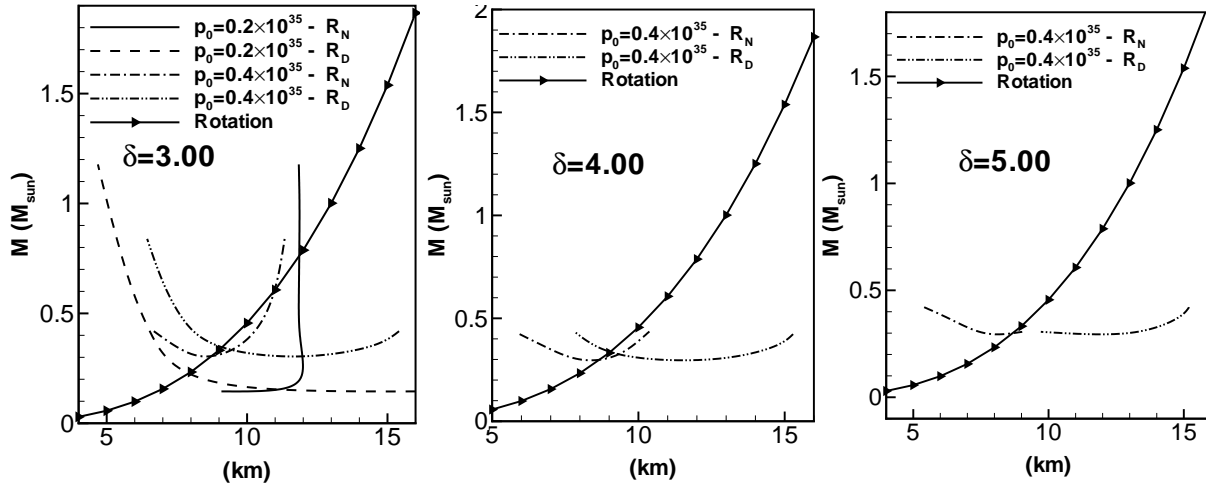
δ	$M_{max}(M_{\odot})$	$R(km)$
0.50	2.06	9.93
0.75	2.06	10.05
1.00	1.16	11.66
2.00	0.89	11.43
3.00	0.84	11.34
4.00	0.42	5.94
5.00	0.42	5.40

with $m = 1.0 \text{ GeV}$ and $\delta \geq 2.00$ we can see that there are low mass DMANSs in which the neutron matter sphere is surrounded by a halo of dark matter consistence with the previous results (Leung & Chu & Lin 2011, 2012). It is evident that with the higher values of δ (for example in stars with $p_0 = 0.4 \times 10^{35} \text{ dyn/cm}^2$ for $\delta \geq 5$), for all stars the neutron matter sphere is surrounded by a halo of dark matter.

Tables 6-8 present the mass and radius of the dark and neutron matter spheres of the maximum mass DMANSs with different DMEOS and for various values of central pressure ratio. We can see that the mass of dark matter sphere

Table 5. Same as Table 3 but for DMANSs with fermionic DMEOS corresponding to $m = 1.0 \text{ GeV}$.

δ	$M_{max}(M_{\odot})$	$R(km)$
0.50	1.95	10.69
0.75	1.88	10.79
1.00	2.01	9.70
2.00	0.85	10.40
3.00	0.53	8.65
4.00	0.58	8.41
5.00	0.56	7.75

**Figure 11.** The total mass versus the neutron (R_N) and dark (R_D) matter sphere radii of DMANSs and the curve that excludes a region by the rotation of 716 Hz pulsar J1748-2446ad (Rotation) with different values of p_0 in dyn/cm^2 unit and central pressure ratio, δ .**Figure 12.** Same as Figure 11 but for other values of central pressure ratio, δ .

increases by increasing the central pressure ratio. This effect is more significant in the case with $p_0 = 0.4 \times 10^{35} \text{ dyn}/\text{cm}^2$. In addition, with this DMEOS the mass of neutron matter sphere reduces as the central pressure ratio grows. In the case with $p_0 = 0.2 \times 10^{35} \text{ dyn}/\text{cm}^2$, for all given values of central pressure ratio the mass of neutron matter sphere is larger than the dark matter sphere. Therefore, the DMANSs are neutron matter dominated in these cases. However, for stars with $p_0 = 0.4 \times 10^{35} \text{ dyn}/\text{cm}^2$ and $\delta \geq 4$ as well as the stars with $m = 1.0 \text{ GeV}$ and $\delta = 5.00$ the dark

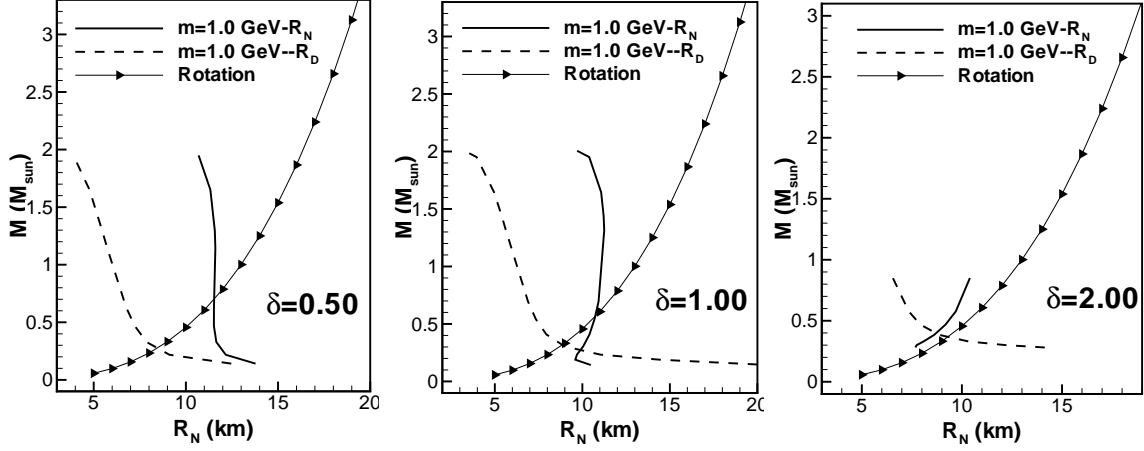


Figure 13. The total mass versus the neutron (R_N) and dark (R_D) matter sphere radii of DMANSs and the curve that excludes a region by the rotation with the fermionic DMEOS for different central pressure ratios, δ .

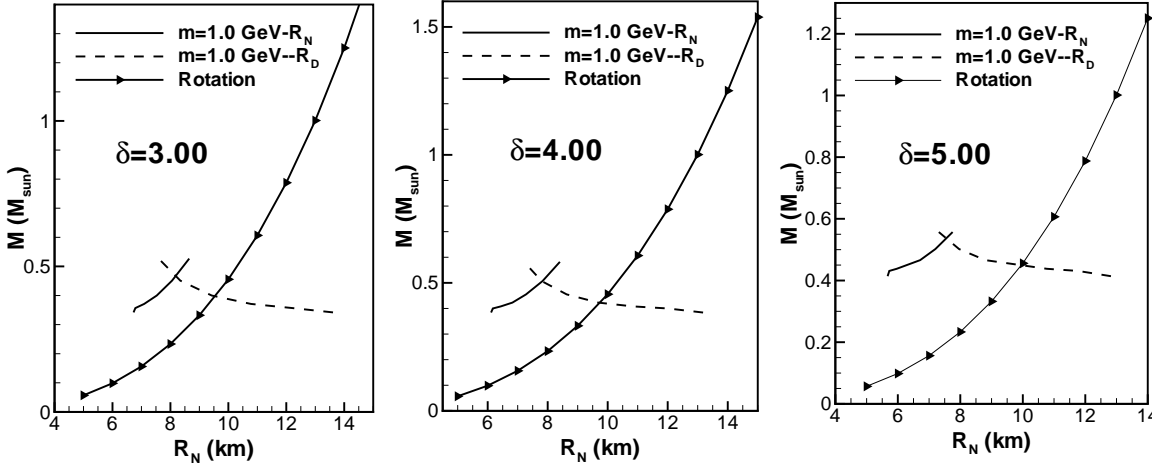


Figure 14. Same as Figure 13 but for other values of central pressure ratio, δ .

Table 6. The mass and radius of the dark and neutron matter spheres of the maximum mass DMANSs with DMEOS corresponding to $p_0 = 0.2 \times 10^{35} \text{ dyn/cm}^2$ for different values of central pressure ratio, δ .

δ	$M_D(M_\odot)$	$R_D(km)$	$M_N(M_\odot)$	$R_N(km)$	$M_{max}(M_\odot)$
0.50	0.01	2.39	2.04	10.44	2.05
0.75	0.01	1.96	2.05	9.811	2.06
1.00	0.02	4.34	1.37	11.80	1.39
2.00	0.02	3.86	1.60	11.59	1.62
3.00	0.03	4.69	1.15	11.84	1.18

matter sphere is heavier than the neutron matter one. Thus, these stars are dark matter dominated. It is obvious from Tables 6-8 that for the neutron dominated DMANSs the halo of dark matter is confined within the neutron matter sphere. This is while in the dark matter dominated DMANSs, the neutron matter sphere is located inside the halo of dark matter which is in agreement with the other investigations (Leung & Chu & Lin 2011, 2012).

Considering two stars with the same mass, one of them a normal neutron star and the other a DMANS in which the neutron matter sphere is surrounded by the halo of dark matter, they have the same gravitational effects due to the same mass. However, the visible radius of the DMANS is smaller than the normal neutron star. Therefore, the gravitational

Table 7. Same as Table 6 but for DMANSs with DMEOS corresponding to $p_0 = 0.4 \times 10^{35} \text{ dyn/cm}^2$.

δ	$M_D(M_\odot)$	$R_D(km)$	$M_N(M_\odot)$	$R_N(km)$	$M_{max}(M_\odot)$
0.50	0.01	2.56	2.05	9.93	2.06
0.75	0.01	2.75	2.05	10.05	2.06
1.00	0.05	5.86	1.11	11.66	1.16
2.00	0.08	6.42	0.81	11.43	0.89
3.00	0.08	6.44	0.76	11.34	0.84
4.00	0.41	15.29	0.01	5.94	0.42
5.00	0.41	15.19	0.01	5.40	0.42

Table 8. Same as Table 6 but for DMANSs with fermionic DMEOS corresponding to $m = 1.0 \text{ GeV}$.

δ	$M_D(M_\odot)$	$R_D(km)$	$M_N(M_\odot)$	$R_N(km)$	$M_{max}(M_\odot)$
0.50	0.04	3.90	1.91	10.69	1.95
0.75	0.06	4.27	1.82	10.79	1.88
1.00	0.05	3.26	1.96	9.70	2.01
2.00	0.18	6.55	0.67	10.40	0.85
3.00	0.25	7.60	0.28	8.65	0.53
4.00	0.28	7.21	0.30	8.41	0.58
5.00	0.31	7.31	0.25	7.75	0.56

redshift of spectral lines can be used to realize these two stars. Figures. 15-18 present the gravitational redshift of normal neutron star and DMANSs with different DMEOSs and various values of central pressure ratio. In all cases, the existence of dark matter leads to higher values of the gravitational redshift compared with the normal neutron stars, in agreement with the previous reports (Xiang et al. 2014; Leung & Chu & Lin 2011). Moreover, the gravitational redshift in the DMANSs with $m = 1.0 \text{ GeV}$ is larger than in the cases with $p_0 = 0.2$ and $p_0 = 0.4 \times 10^{35} \text{ dyn/cm}^2$. Figures. 15-18 indicate that the effects of dark matter on the gravitational redshift are more significant in stars with the higher values of δ . These results can be used to distinguish the normal neutron stars from DMANSs with different DMEOSs and contributions of dark matter.

4. SUMMARY AND CONCLUSIONS

Applying the dark matter equations of state (DMEOSs) from the rotation curves of galaxies as well as the fermionic DMEOS with $m = 1.0 \text{ GeV}$ and the neutron matter equation of state from Skyrme effective force, we have studied the structure of dark-matter admixed neutron stars (DMANSs). We have found that the radius of a DMANS is smaller than the radius of a normal neutron star with the same mass. Our results show that the mass-radius relations are affected by both DMEOS and central pressure of dark matter to neutron matter ratio. Specifically, depending on the DMEOS and the central pressure ratio, the DMANS can be gravitationally or self bound star. Additionally, it has been confirmed that in some cases two DMANSs with equal visible radii but different masses can exist. This fact is a consequence of different degrees of dark matter domination in DMANS. We have shown that with all DMEOSs, the maximum mass of DMANS is lower than the normal neutron star. The observed neutron stars EXO 1745-248, 4U 1608-52, and 4U 1820-30 which are inconsistent with the previous observations and theoretical properties of normal neutron stars can be explained with our model. We have confirmed that some DMEOSs and central pressure ratios considered in this work result in the dark matter dominated neutron stars with a halo of dark matter around a small neutron matter sphere. Our calculations suggest that the observed neutron stars EXO 1745-248, 4U 1608-52, and 4U 1820-30 may be dark matter dominated neutron stars. It has been clarified that the radius of the neutron matter sphere decreases while the radius of the dark matter sphere increases as the central pressure ratio grows. Besides, the

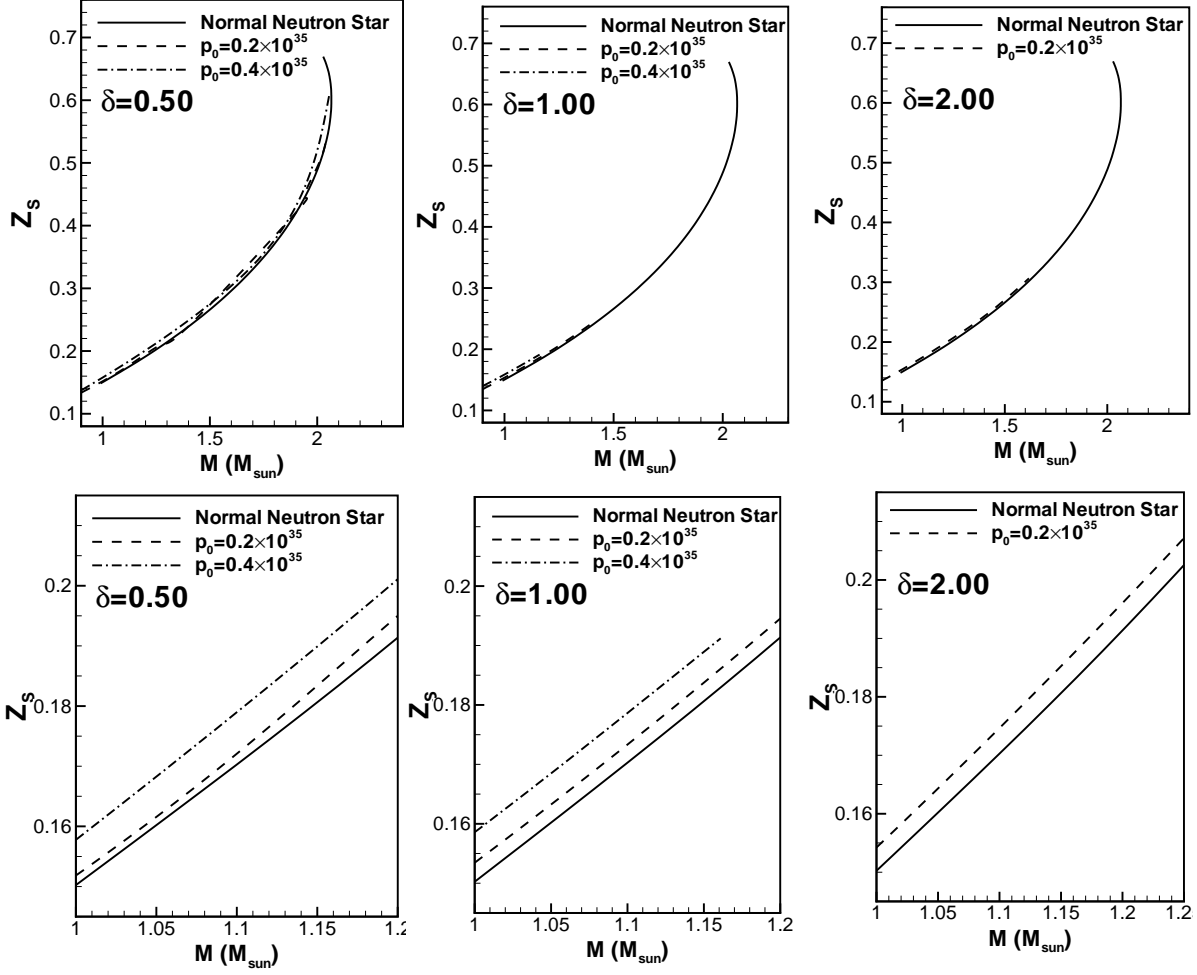


Figure 15. Top: gravitational redshift, Z_s , versus total mass of DMANSs with different DMEOSs from the velocity profile of galaxies and central pressure ratio, δ . Bottom: same as top, but for a different range of DMANS mass.

mass of the dark matter sphere increases with the increase in the central pressure ratio. Moreover, the DMANSs with high values of the central pressure ratio are dark matter dominated neutron stars. Finally, we have shown that the existence of dark matter in the DMANSs results in the increase of the gravitational redshift.

The author wish to thank the Shiraz University Research Council.

REFERENCES

- Akmal, A., & Pandharipande, V.R. 1997, Phys. Rev. C, 56, 2261
 Alford M., et al. 2007, Nature, 445, E7
 Antoniadis J., et al. 2013, Science, 340, 448
 Ade P. A. R., et al. 2014, ArXiv e-prints: 1303.5076v1
 Baym G., Pethick C., & Sutherland P. 1971, ApJ, 170, 299
 Bertone G., & Fairbairn M. 2008, Phys. Rev. D, 77, 043515
 Barranco J., Bernal A., & Nunez D. 2015, MNRAS, 449, 403
 Chabanat E., et al. 1997, Nuc. Phys. A, 627, 710
 Ciarcelluti P., & Sandin F. 2011, Phys. Lett. B, 695, 19
 Demorest P., et al. 2010, Nature, 467, 1081
 Engvik, L., et al. 1994, Phys. Rev. Lett., 73, 2650
 Fuller J., & Ott C. 2015, MNRAS, L71
 Goldman I., & Nussinov S. 1989, Phys. Rev. D, 40, 3221
 Guver T., et al. 2010, ApJ, 712, 964
 Guver T., et al. 2010, ApJ, 719, 1807
 Kouvaris C. 2008, Phys. Rev. D, 77, 023006
 Kouvaris C. 2012, Phys. Rev. Lett., 108, 191301
 Klahn T., et al. 2007, Phys. Lett. B, 654, 170
 Lattimer J. M., & Prakash M. 2001, ApJ, 550, 426
 Lattimer J. M. & Prakash M. 2007, Phys. Rep., 442, 109
 Lavallaz A. D., & Fairbairn M. 2010, Phys. Rev. D, 81, 123521
 Li A., et al. 2010, Phys. Rev. C, 81, 025806
 Leung S.-C., Chu M.-C., & Lin L.-M. 2011, Phys. Rev. D, 84, 107301
 Leung S.-C., Chu M.-C., & Lin L.-M. 2012, Phys. Rev. D, 85, 103528
 Li A., Huang F., & Xu R.-X. 2012, Astropart. Phys., 37, 70
 Massey R., et al. 2007, Nature, 445, 286
 Narain G., Schaffner-Bielich J., & Mishustin I. N. 2006, Phys. Rev. C, 74, 063003

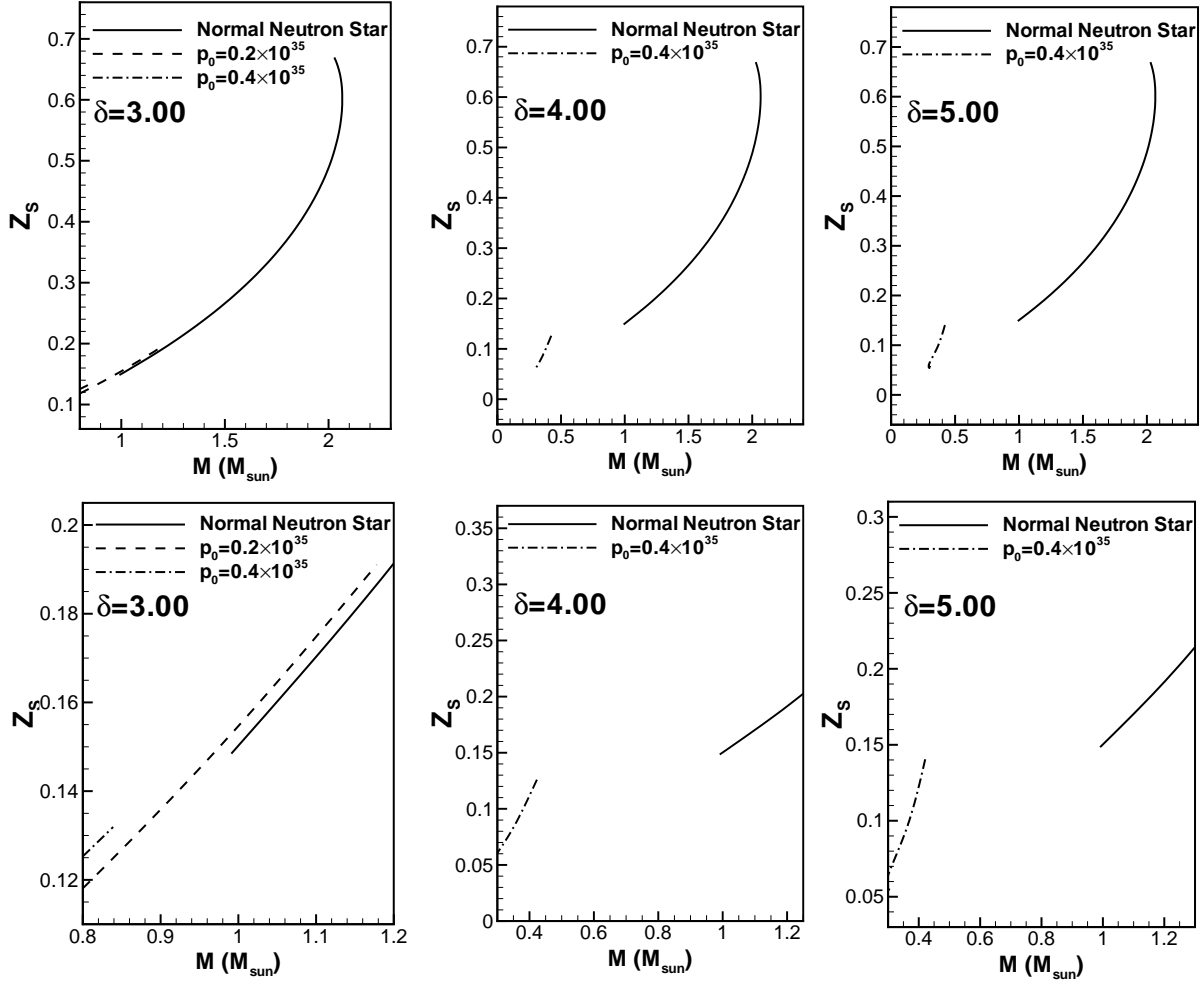


Figure 16. Same as Figure 15 but for other values of central pressure ratio, δ .

Ozel F. 2006, Nature, 441, 1115
 Ozel F., Guver T., & Psaltis D. 2009, ApJ, 693, 1775
 Page D. & Reddy S. 2006, Ann. Rev. Nucl. Part. Sci., 56, 327
 Perez-Garcia M. A., Silk J., & Stone J. R. 2010, Phys. Rev. Lett., 105, 141101
 Perez-Garcia M. A., & Silk J. 2012, Phys. Lett. B, 711, 6
 Prakash, M., Ainsworth, T.L. & Lattimer, J.M. 1988, Phys. Rev. Lett., 61, 2518
 Springel V., et al. 2005, Nature, 435, 629

Sandin F., & Ciarcelluti P. 2009, Astropart. Phys., 32, 278
 Serra A. L., & Dominguez Romero M. J. L. 2011, MNRAS, 415, L74
 Weber F. 2005, Prog. Part. Nucl. Phys., 54, 193
 Weber M., & de Boer W. 2010, A & A, 509, A25
 Xiang Q.-F., et al. 2014, Phys. Rev. C, 89, 025803

ALL AUTHORS AND AFFILIATIONS

AND

Z. REZAEI.

Physics Department and Biruni Observatory
 College of Sciences, Shiraz University
 Shiraz 71454, Iran

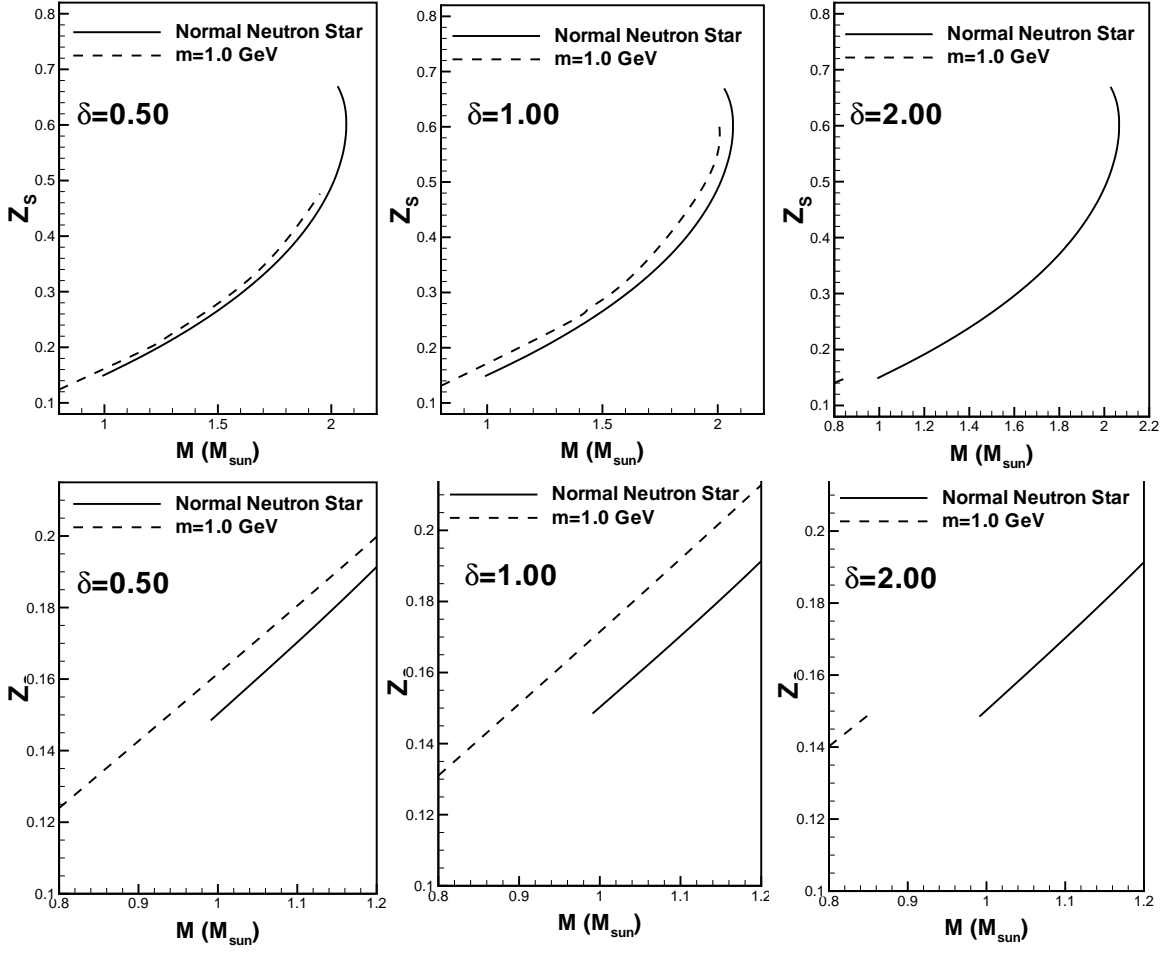


Figure 17. Same as Figure 15 but for DMANSs with the fermionic DMEOS for different central pressure ratios, δ .

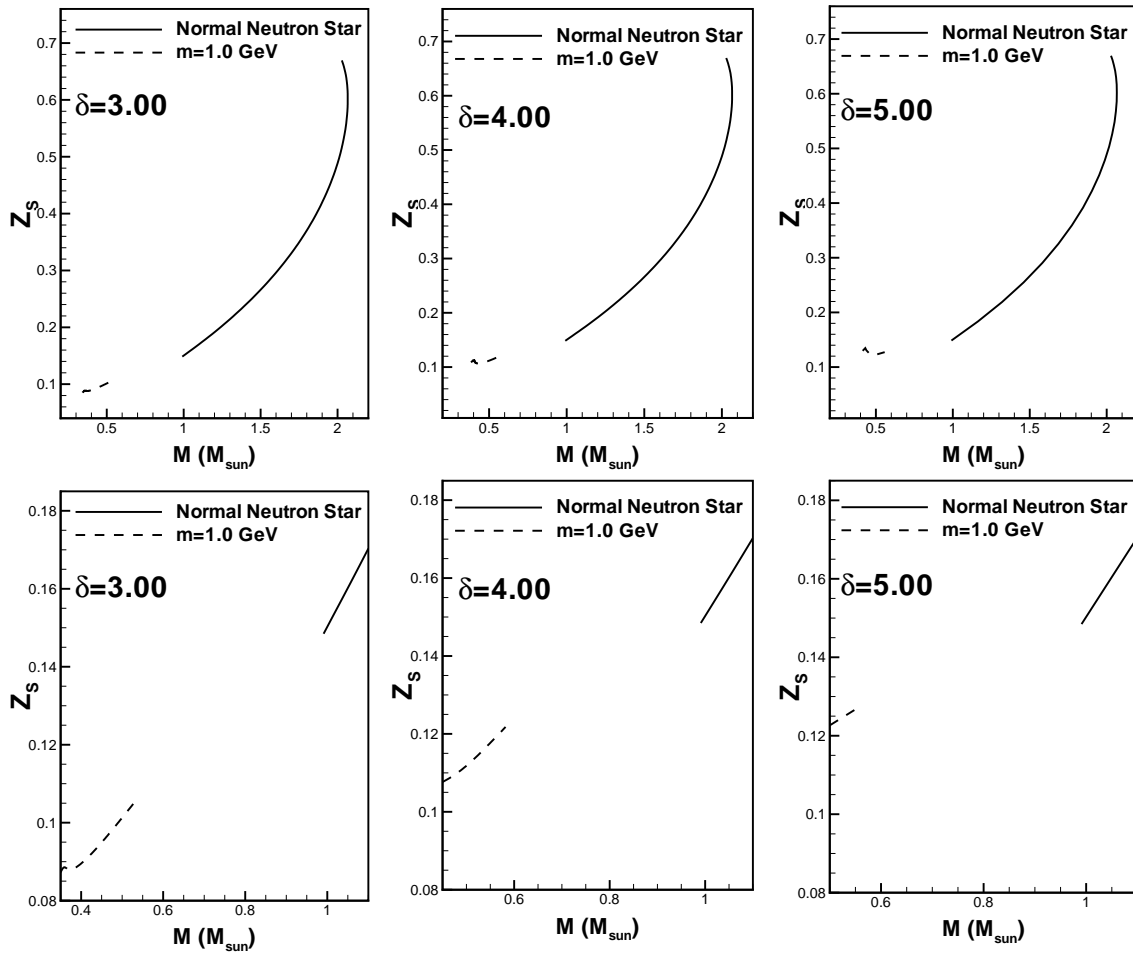


Figure 18. Same as Figure 17 but for other values of central pressure ratio, δ .